

DYNAMICAL GENERATION OF THE GAUGED SU(2) LINEAR SIGMA MODEL*

R. DELBOURGO and M. D. SCADRON†

Physics Department, University of Tasmania, Hobart, Australia 7005

15 October 1993

Abstract

The fermion and meson sectors of the quark-level SU(2) linear sigma model are dynamically generated from a meson-quark Lagrangian, with the quark (q) and meson (σ , $\vec{\pi}$) fields all treated as elementary, having neither bare masses nor expectation values. In the chiral limit, the masses are predicted to be $m_q = f_\pi g$, $m_\pi = 0$, $m_\sigma = 2m_q$, and we also find that the quark-meson coupling is $g = 2\pi/\sqrt{N_c}$, the three-meson coupling is $g' = m_\sigma^2/2f_\pi = 2gm_q$ and the four-meson coupling is $\lambda = 2g^2 = g'/f_\pi$, where $f_\pi \simeq 90$ MeV is the pion decay constant and $N_c = 3$ is the colour number. By gauging this model one can generate the couplings to the vector mesons ρ and A_1 , including the quark-vector coupling constant $g_\rho = 2\pi$, $g_{\rho\pi\pi}$, $g_{A_1\rho\pi}$ and the masses $m_\rho \sim 700$ MeV, $m_{A_1} \simeq \sqrt{3}m_\rho$; of course the vector and axial currents remain conserved throughout.

1 Introduction

Although quantum chromodynamics (QCD) may indeed be the correct chiral-invariant field theory of strong interactions, it is quite difficult to quantify in the low-energy region. As an alternative, one may consider effective chiral theories which presumably simulate QCD in the infrared domain. Focussing on an isospin group, we will specifically consider 0^{-+} pseudoscalars ($\vec{\pi}$), 0^{++} scalars (σ), 1^{--} vectors ($\vec{\rho}$) and 1^{++} axial vectors (\vec{A}_1). Weinberg [1] has recently reemphasized the importance of treating all four of these chiral sectors in a global context.

It is by now legend that the SU(2) linear sigma model (LSM) of Gell-Mann and Levy [2], with elementary nucleons, sigma and pion fields, is the prototype

*Published in *Mod. Phys. Lett.* **A10** (1995) 251.

†Permanent address: Physics Department, University of Arizona, Tucson, AZ 85721, USA

field theory characterizing spontaneously broken chiral symmetry. Likewise the four-fermion (quark) field theory of Nambu and Jona-Lasinio (NJL [3]), generating the chiral-limiting (CL) bound state $\bar{q}q$ meson masses,

$$m_\pi = 0, \quad m_\sigma = 2m_q, \quad (1)$$

where m_q is the quark mass, is the classic example of dynamically broken chiral symmetry. These two field theories appear to be different in as much as the nucleon level LSM does not constrain the scalar mass m_σ as does Eq. (1), although the masslessness of the Goldstone field $\vec{\pi}$ is certainly preserved in both cases.

However, if one formulates the SU(2) LSM *at the quark level*, it has been suggested [4] that with spontaneous breaking the theory may be identical to the dynamically broken NJL model, for $N_c = 3$. In fact, the one-loop order LSM not only recovers (1), but it also leads to many more low-energy theorems [5, 6], known to hold in tree order [7]. Notwithstanding the above successes, a spontaneously broken LSM still appears fundamentally different from the dynamically broken NJL theory, especially in its *effective description* of low-energy QCD.

In this paper, in sections 2 and 3, we will dynamically generate the LSM at the quark level in the spirit of NJL. Unlike others [8] this will be done in the self-consistent sense that *bare masses and expectation values vanish*,

$$0 = m_{q0} = \langle \vec{\pi}_0 \rangle = \langle \sigma_0 \rangle,$$

signifying that the dynamically induced quantities m_q and $\langle \sigma \rangle = -f_\pi$ obey $\delta m_q = m_q, \delta f_\pi = f_\pi$. We will likewise induce the cubic and quartic meson couplings by the same non-perturbative bootstrap. Thus for our starting chiral quark model (CQM) Lagrangian we take

$$\mathcal{L} = \bar{\psi}[i\gamma \cdot \partial + g(\sigma + i\vec{\tau} \cdot \vec{\pi} \gamma_5)]\psi + [(\partial\sigma)^2 + (\partial\vec{\pi})^2]/2, \quad (2)$$

where σ and π are scalar and pseudoscalar meson fields and the quark spinor ψ corresponds to an up-down doublet coming in N_c colours.

Following the approach of NJL, we induce a non-perturbative quark mass m_q by anticipating a mass gap equation $\delta m_q = m_q$ through a quark loop, which also induces the pion decay constant. In this way the associated axial vector current for the (now massive) free quarks,

$$\vec{\mathcal{A}}_\mu = \bar{\psi}\gamma_\mu\gamma_5\vec{\tau}\psi/2 + if_\pi g(\partial_\mu/\partial^2)\bar{\psi}\gamma_5\vec{\tau}\psi, \quad (3)$$

develops a pseudoscalar pole and remains conserved in the chiral limit (CL), $\partial^\mu \vec{\mathcal{A}}_\mu = 0$. Of course the Goldstone pion [9] remains massless and the Goldberger-Treiman (GT) relation must hold at the quark level, $f_\pi g = m_q$ to ensure axial current conservation. The CL non-perturbative pion decay constant $f_\pi \simeq 90$ MeV arises from the definition $\langle 0|\mathcal{A}_\mu^j(0)|\pi^k(q)\rangle = i\delta^{jk}f_\pi q_\mu$ and g is nothing but the dimensionless meson-quark coupling appearing in (2).

Then in section 4 we gauge the chiral quark model (2) to include vector and axial-vector couplings and masses in the theory. Finally, in section 5, we give a dynamically generated LSM interpretation of the very successful phenomenology of vector meson dominance. The results are summarized in section 6.

2 Generating the sigma model

In the NJL model, the mass gap and binding equations are equivalent but both are quadratically divergent. However, in our quark-meson CQM scheme (2), the one-loop graph of Fig. 1a which induces f_π is logarithmically divergent, whereas the mass gap equation of Fig. 1b is quadratically divergent [10] In the former case we obtain in the soft limit [11]

$$f_\pi = -4iN_c g m_q \int \bar{d}^4 p / (p^2 - m_q^2)^2.$$

Substituting the GT relation, the quark mass $m_q \neq 0$ cancels out, leading to the logarithmically divergent equation,

$$1 = -4iN_c g^2 \int \frac{\bar{d}^4 p}{(p^2 - m_q^2)^2}. \quad (4)$$

This “gap equation” (4) is compatible with a cutoff approach, as we will show later. With the quadratically divergent mass gap equation, depicted by the quark tadpole graph of Fig. 1b, the condition $\delta m_q = m_q$ (or $m_0 = 0$) yields [11, 12],

$$m_q = -\frac{8iN_c g^2}{m_\sigma^2} \int \frac{\bar{d}^4 p}{p^2 - m_q^2} \frac{m_q}{p^2 - m_q^2}. \quad (5)$$

However it is dangerous to introduce an ultraviolet cut-off in a *quadratically* divergent graph since this depends sensitively on shift of origin; in fact attempting to do so above produces an imaginary g . Moreover since m_q does not appear in our initial CQM lagrangian (2), one could shift the σ field to $\sigma \rightarrow \sigma - f_\pi$ so that (2) acquires a chiral-broken kinetic part $\bar{\psi}(i \not{\partial} - f_\pi g)\psi$ with $f_\pi g = m_q$. If the latter mass is to be identified with the quark tadpole of Fig 1b, it must be a counter-term mass of opposite sign [12] (relative to standard Feynman rules or to mass renormalization involving a cutoff) in order that the original σ field is unshifted as in (2).

Instead we shall henceforth appeal to dimensionless regularization [13] and make no reference to a cutoff. This gives in $2l$ -dimensions,

$$\begin{aligned} \int \bar{d}^{2l} p / (p^2 - m^2)^2 &= i\Gamma(2-l)(m^2)^{l-2}/(4\pi)^l, \\ \int \bar{d}^{2l} p / (p^2 - m^2) &= -i\Gamma(1-l)(m^2)^{l-1}/(4\pi)^l. \end{aligned}$$

Therefore in the four-dimensional limit, one obtains the finite difference,

$$\int \bar{d}^4 p \left[\frac{m^2}{(p^2 - m^2)^2} - \frac{1}{p^2 - m^2} \right] = \lim_{l \rightarrow 2} \frac{im^{2l-2}}{(4\pi)^2} [\Gamma(2-l) + \Gamma(1-l)] = -\frac{im^2}{(4\pi)^2}. \quad (6)$$

This lemma (6) allows us to express the quadratic divergence in (5) in terms of a logarithmic one and gives

$$m_q = -\frac{8iN_c g^2}{m_\sigma^2} \int \frac{m_q \bar{d}^4 p}{p^2 - m_q^2} = -\frac{8im_q N_c g^2}{m_\sigma^2} \left[\int \frac{m_q^2 \bar{d}^4 p}{(p^2 - m_q^2)^2} + i \frac{m_q^2}{16\pi^2} \right],$$

$$\text{or} \quad 1 = ac2m_q^2 m_\sigma^2 \left[1 + \frac{g^2 N_c}{4\pi^2} \right]. \quad (7)$$

Note that the sign change of the gamma function sum in (6) in turn cancels the minus sign of the counter-term quark mass in (5). In short the lemma (6) renders the mass gap equation (5) compatible with (4), since both terms in (7) are positive definite.

Next we examine the meson self-energies to one-loop order, depicted in Figs. 2a, 2b and 3a, 3b. Given \mathcal{L} in (2), the pion self-mass bubble and tadpole graphs are both quadratically divergent but their coefficients precisely cancel, as required by the Goldstone theorem [5, 9],

$$m_\pi^2 = 4iN_c [2g^2 - 4gg'm_q/m_\sigma^2] \int \bar{d}^4 p / (p^2 - m_q^2) = 0, \quad (8)$$

provided we dynamically require a $\sigma\pi\pi$ coupling $g' = m_\sigma^2/2f_\pi$. This is just what the Gell-Mann-Levy model stipulates, independently of the m_σ scale.

The analogous scalar meson self-energy graphs of Figs. 3a, 3b can also be handled by dimensional regularization, in contrast to the approach of refs. [6]. Although m_σ also does not appear in the primary CQM lagrangian (2), the shifted nonzero $\langle\sigma\rangle$ will induce an m_σ via Figs 3 but with $m_q \neq 0$ in the quark loops. Again using a counter-term m_σ^2 in the dimensionless regularization approach [12], the unshifted lagrangian (2) dynamically generates a scalar mass $m_\sigma \neq 0$. In particular, including the 3σ Feynman combinatoric factor [14] of $3!$, the CL sum of the scalar meson tadpole and bubble graphs of Figs. 3a, 3b gives [15],

$$m_\sigma^2 = 8iN_c g^2 \int \bar{d}^4 p \frac{(p^2 + m_q^2)}{(p^2 - m_q^2)^2} - 48iN_c \frac{gg'm_q}{m_\sigma^2} \int \frac{\bar{d}^4 p}{p^2 - m_q^2}.$$

Using the finite difference (6) and the same CL relation $g' = m_\sigma^2/2f_\pi$, we find

$$m_\sigma^2 = 16iN_c g^2 \left[\int \frac{m_q^2 \bar{d}^4 p}{(p^2 - m_q^2)^2} - \int \frac{\bar{d}^4 p}{p^2 - m_q^2} \right] = \frac{N_c g^2 m_q^2}{\pi^2}. \quad (9)$$

Solving the two identities (7) and (9), we discover that the NJL mass $m_\sigma = 2m_q$ has been dynamically generated and that the meson-quark coupling constant is determined to be $g = 2\pi/\sqrt{N_c}$.

3 Higher point functions to 1-loop order

Proceeding to the 3-point functions induced by the quark loop, the CQM Lagrangian (2) dynamically generates the graphs of Figs. 4a, 4b. In the zero momentum CL we obtain [15]

$$g_{\sigma\pi\pi} = -8ig^3 N_c m_q \int \frac{\bar{d}^4 p}{(p^2 - m_q^2)^2} = 2gm_q, \quad (10)$$

upon using Eq. (4). Similarly, in the chiral limit,

$$g_{\sigma\sigma\sigma} = -8ig^3 N_c \int \frac{3p^2 m_q + m_q^3}{(p^2 - m_q^2)^3} \bar{d}^4 p = 6gm_q, \quad (11)$$

where we have just retained the dominant logarithmically divergent piece. These results accord perfectly with the tree coupling relations (for $m_\sigma = 2m_q$),

$$2gm_q = m_\sigma^2/2f_\pi = g' \quad (12)$$

associated with the interaction $g'\sigma(\sigma^2 + \vec{\pi}^2)$, including the Feynman symmetry factors. The only point of note is that the cubic couplings have been derived in a bootstrapped manner in as much as “loops reproduce trees”. These bootstrap concepts have a direct affinity with renormalization conditions [16] $Z = 0$ appropriate to particles which are not elementary, but bound states of more basic fields.

Finally we generate the quartic meson-meson couplings dynamically [15]. The Feynman graphs of Fig. 5 arising from (2) lead to logarithmically divergent integrals⁶ for which we use equation (4) again:

$$\begin{aligned} -2g^2 &= 8iN_c g^4 \int \frac{\bar{d}^4 p}{(p^2 - m_q^2)^2} \\ &= g_{\sigma\sigma\sigma\sigma}/6 = g_{\pi\pi\pi\pi}/6 = g_{\sigma\sigma\pi\pi}/2. \end{aligned} \quad (13)$$

This can be interpreted perfectly as an interaction $-\lambda(\sigma^2 + \vec{\pi}^2)^2/4$ where

$$\lambda = 2g^2 = g'/f_\pi. \quad (14)$$

Thus the quark loop of Fig.5 also bootstraps to a tree and generates the quartic meson couplings dynamically.

Collecting our various results, we have established that with the non-perturbative generation of the quark mass and pion decay constant, connected by $m_q = f_\pi g$,

there are induced dynamically the meson masses $m_\pi = 0$, $m_\sigma = 2m_q$ and the meson interactions

$$g'\sigma(\sigma^2 + \bar{\pi}^2) - (\lambda/4)(\sigma^2 + \bar{\pi}^2)^2$$

for $\lambda = 2g^2$, together with the original meson-quark interaction

$$g\bar{\psi}(\sigma + i\gamma_5\vec{\tau}\cdot\vec{\pi})\psi,$$

with $g' = m_\sigma^2/2f_\pi = 2gm_q$. This is identical in form with the model of Gell-Mann-Levy, except that now the mass of the scalar meson is dynamically fixed to the NJL value in (1) and the strong coupling for $N_c = 3$ is also fixed to be

$$g = 2\pi/\sqrt{N_c} = 3.6276, \quad (15)$$

which is compatible with the ratio $m_q/f_\pi \simeq 3.6$, arising from the GT relation. Alternatively, making use of the experimental $g_{\pi NN} \simeq 13.4$ in $N = qq\bar{q}$ and [17] $g_A = 1.2573$, we may estimate $g = g_{\pi NN}/3g_A \simeq 3.55$. The mass values also make good sense since the CL constituent quark mass is dynamically fixed to be $m_q = 2\pi f_\pi/\sqrt{3} \simeq 325$ MeV, as might be expected for a constituent quark. Lastly, the NJL σ mass is $m_\sigma = 2m_q \simeq 650$ MeV in the chiral limit, not incompatible with observational signals [18].

Notwithstanding the impressive self-consistency of the scheme, we have one final constraint to consider: because we have worked around the true vacuum, we must verify that the chiral-symmetric vacuum expectation values are satisfied. This means that we must check Lee's [14] null tadpole condition, taking into account the induced meson interactions. Evaluating the graphs of Fig. 6, in the language of dimensional regularization, we must verify that [11] the tadpole *sum* vanishes:

$$\langle\sigma'\rangle = 0 = -8iN_cgm_q \int \frac{\bar{d}^{2l}p}{p^2 - m_q^2} + 3ig' \int \frac{\bar{d}^{2l}p}{p^2} + 3ig' \int \frac{\bar{d}^{2l}p}{p^2 - m_\sigma^2}. \quad (16)$$

The first and third integrals in (16) scale respectively to m_q^2 and m_σ^2 and of course we discard the massless tadpole in dimensional regularization. Hence we find as $l \rightarrow 2$ that a cancellation of the pole terms will occur providing

$$N_c(2m_q)^4 = 3m_\sigma^4. \quad (17)$$

Curiously, this seems to require that there be three colours, $N_c = 3$ for two flavours. This conclusion parallels the chiral anomaly [19] prediction of the $\pi^0 \rightarrow 2\gamma$ quark loop amplitude in the chiral limit [20],

$$F_{\pi^0\gamma\gamma} = \alpha N_c/3\pi f_\pi, \quad (18)$$

which leads to a decay rate (for 3 colours and 2 flavours) of

$$\Gamma_{\pi^0\gamma\gamma} = m_\pi^3 |F_{\pi^0\gamma\gamma}|^2/64\pi \simeq 7.63 \text{ eV}, \quad (19)$$

quite close [17] to the measured value of $7.74 \pm .55$ eV. Note that using a quark loop, rather than a nucleon loop [21], the successful rate (19) can also be regarded as an LSM prediction.

Stated another way, in the CQM field theory, the NJL relation $m_\sigma = 2m_q$ is initially generated via the quark mass gap of Figure 1b. However the consequent $Z = 0$ vertex condition helps to induce dynamically the linear sigma model field theory, starting with (2). At that level one obtains a vacuum expectation value for the full σ field (not the bare σ_0) as $\langle \sigma \rangle = -f_\pi$. One then shifts to σ' as $\sigma = \sigma' + \langle \sigma \rangle = \sigma' - f_\pi$. This corresponds to adding “zero” 3-point terms to the Lagrangian (2) of the type $Z_{g'}\sigma'(\sigma'^2 + \vec{\pi}^2)$ with compositeness condition $Z_{g'} = 0$. One thereby obtains the renormalized Lagrangian,

$$\mathcal{L} = \bar{\psi}(i\gamma \cdot \partial - m_q)\psi + g\bar{\psi}(\sigma' + i\gamma_5 \vec{\tau} \cdot \vec{\pi})\psi + g'\sigma'(\sigma'^2 + \vec{\pi}^2) + (Z_{g'} - 1)g'\sigma'(\sigma'^2 + \vec{\pi}^2) + ..$$

where the dots refer to “zero” 4-point Lagrangian terms. As usual one determines the vertex renormalization constant $Z_{g'}$ by evaluating the perturbative sum of 3-point plus quark loop graphs and thus recovers Eqns. (10) and (11) upon setting $Z_{g'} = 0$. Note that the above renormalized CQM Lagrangian “knows” about the meson terms such as the trilinear ones.

If instead we dynamically induce the entire linear sigma model, then the quark mass gap graph of Fig. 1b must be supplemented by σ' - and $\vec{\pi}$ - mediated quark self-energies and also σ' and π tadpole graphs, which then all sum to zero. In this scenario the NJL mass relation $m_\sigma = 2m_q$ is a consequence of the Lee constraint $\langle \sigma' \rangle = 0$, or Eqns. (16) and (17). Then because (18) empirically fixes $N_c = 3$, one sees from (17) that the NJL mass relation follows.

Thus far we have consistently adopted only one regularization scheme, dimensional regularization. Nevertheless a cutoff version of (4) would replace the right-hand side (rhs) by $\ln(1 + \Lambda^2/m_q^2) - \Lambda^2(\Lambda^2 + m_q^2)^{-1}$. Setting the latter to unity in turn suggests $\Lambda/m_q \simeq 2.3$ or $\Lambda \simeq 750$ MeV for $m_q = 2\pi f_\pi/\sqrt{3} \simeq 325$ MeV. This cutoff sensibly separates the elementary quarks and mesons from the known higher-mass $\bar{q}q$ SU(2) bound states at $\rho(770)$, $\omega(783)$, $A_1(1260)$, etc.

A few concluding remarks are called for. It is also possible to construct an effective LSM potential following the method of Coleman and Weinberg [22] but that scheme does not require the conditions

$m_\sigma = 2m_q$ or $g = 2\pi/\sqrt{3}$, although we should mention that a combined LSM-NJL picture [23] has recently been linked to low-energy QCD.

4 Generating the vector masses and couplings

We now make the chiral quark model (CQM) Lagrangian (2) invariant under *local* SU(2) \times SU(2) by gauging the entire structure. In the standard way one replaces ordinary derivatives by covariant derivatives,

$$D\psi = [\partial + ig_\rho(\vec{V} - \vec{A}_{\gamma_5}) \cdot \vec{\tau} + ieV^{em}]\psi, \quad (20)$$

$$D\sigma = \partial\sigma - 2g_\rho \vec{A} \cdot \vec{\pi}, \quad D\vec{\pi} = \partial\vec{\pi} + 2g_\rho(\vec{\rho} \times \vec{\pi} + \vec{A}\sigma), \quad (21)$$

and then writes down the (massless) gauge-invariant Lagrangian

$$\mathcal{L} = \bar{\psi}[i\gamma \cdot D + g(\sigma + i\gamma_5 \vec{\tau} \cdot \vec{\pi})]\psi + [(D\sigma)^2 + (D\vec{\pi})^2]/2 - [\vec{F}_V^2 + \vec{F}_A^2]/4; \quad (22)$$

$$\vec{F}_{\mu\nu}^V = \partial_\mu \vec{\rho}_\nu - \partial_\nu \vec{\rho}_\mu + 2g_\rho(\vec{\rho}_\mu \times \vec{\rho}_\nu + \vec{A}_\mu \times \vec{A}_\nu), \quad (23)$$

$$\vec{F}_{\mu\nu}^A = \partial_\mu \vec{A}_\nu - \partial_\nu \vec{A}_\mu + 2g_\rho(\vec{\rho}_\mu \times \vec{A}_\nu + \vec{A}_\mu \times \vec{\rho}_\nu). \quad (24)$$

Even though the σ meson and both u and d quarks acquire masses, the vector and axial currents of course remain conserved, leading to gauge-invariant kinematic structures in amplitudes. Nevertheless we will show that the full propagators of the vector and axial gauge fields (ρ and A_1) develop poles at finite masses through the contributions of quark and meson loops.

But first we dynamically induce the gauge coupling constant g_ρ in (20,21). This comes about through the vector current matrix element

$$\langle 0 | \mathcal{V}_\mu^{em} | \rho^0(k) \rangle = ek^2 \epsilon_\mu(k) / g_\rho; \quad k^2 = m_\rho^2, \quad (25)$$

represented by the quark loop in Fig. 7 which evaluates to

$$\langle 0 | \mathcal{V}_\mu^{em} | \rho_\nu^0(k) \rangle = -eg_\rho \Pi_{\mu\nu}(k^2, m_q^2) = eg_\rho(k^2 g_{\mu\nu} - k_\mu k_\nu) \Pi(k^2, m_q^2), \quad (26)$$

with

$$\Pi(k^2, m^2) = -8iN_c \int_0^1 d\alpha \int \bar{d}^4 p \quad \alpha(1-\alpha)/[p^2 - m^2 + k^2\alpha(1-\alpha)]^2. \quad (27)$$

Proceeding to the soft (chiral) limit in the invariant amplitude (27), one is led to

$$\frac{1}{g_\rho^2} = \Pi(0, m_q^2) = -\frac{8iN_c}{6} \int \frac{\bar{d}^4 p}{(p^2 - m_q^2)^2} = \frac{1}{3g^2}, \quad (28)$$

upon employing the gap equation (4). However, we already know that with three colours, $g = 2\pi/\sqrt{3}$, so we deduce that in the chiral limit,

$$g_\rho = \sqrt{3}g = 2\pi. \quad (29)$$

This result has already been obtained by other methods [24].

Although (29) roughly approximates the data, one must admit that it is 50% too large since the observed $\rho \rightarrow e\bar{e}$ rate gives $g_\rho^2/4\pi \simeq 2.01$. It indicates that we may improve on our analysis by moving away from the soft chiral limit to the real ρ mass shell. By this subtraction procedure we arrive at a better approximation,

$$\frac{1}{g_\rho^2} - \frac{1}{4\pi^2} = \Pi(m_\rho^2, m_q^2) - \Pi(0, m_q^2)$$

$$= -8iN_c \int_0^1 \alpha(1-\alpha) d\alpha \int \left[\frac{\bar{d}^4 p}{[p^2 - m_q^2 + m_\rho^2 \alpha(1-\alpha)]^2} - \frac{\bar{d}^4 p}{[p^2 - m_q^2]^2} \right]. \quad (30)$$

To be consistent with the gap equation (4), cut-off at Λ so that

$$1 = \ln(1 + \Lambda^2/m_q^2) - 1/(1 + m_q^2/\Lambda^2), \quad (31)$$

yielding $\Lambda \simeq 750$ MeV for $m_q \simeq 325$ MeV, we reexpress (31) for $N_c = 3$ as

$$\begin{aligned} \frac{1}{g_\rho^2} - \frac{1}{4\pi^2} = \frac{3}{2\pi^2} \int_0^1 \alpha(1-\alpha) d\alpha \left[\ln \left(1 + \frac{\Lambda^2}{m_q^2 - m_\rho^2 \alpha(1-\alpha)} \right) - \ln \left(1 + \frac{\Lambda^2}{m_q^2} \right) \right. \\ \left. - \frac{\Lambda^2}{\Lambda^2 + m_q^2 - m_\rho^2 \alpha(1-\alpha)} + \frac{\Lambda^2}{\Lambda^2 + m_q^2} \right]. \quad (32) \end{aligned}$$

Assuming that $m_\rho \sim \Lambda \sim 750$ MeV, we can estimate the integrals on the rhs of (32) quite well by using the mean value $\overline{\alpha(1-\alpha)} = 1/6$. In this way we find $g_\rho^{-2} - (2\pi)^{-2} \simeq 0.46(2\pi)^{-2}$ or $g_\rho^2/4\pi \simeq 2.15$, much closer to the experimental value.

The quark-meson coupling g_ρ determines the $\rho\pi\pi$ and other couplings through the gauge principle as Eqs. (21) and (22) readily show:

$$\mathcal{L} \supset 2g_\rho(\vec{\rho}^\mu \times \vec{\pi} \cdot \partial_\mu \vec{\pi} + \sigma \vec{A}^\mu \cdot \partial_\mu \vec{\pi} + g_\rho \sigma^2 \vec{A}_\mu \cdot \vec{A}^\mu + 2g_\rho \sigma \vec{\rho}_\mu \times \vec{\pi} \cdot \vec{A}^\mu) + \dots \quad (33)$$

However it is very interesting and important to check that the meson interactions are also consistently determined by the quark loops as in Fig. 8. A simple calculation of those diagrams shows that in the chiral limit [5]

$$g_{\rho\pi\pi} = -4ig^2 g_\rho N_c \int \bar{d}^4 p / (p^2 - m_q^2)^2 = g_\rho, \quad (34)$$

using the gap equation (4). Of course (34) also conforms to vector meson dominance (VMD) universality [25], which is approximately valid [26]. The bootstrapping (34) of the $g_{\rho\pi\pi}$ coupling can also be interpreted as a vertex renormalization condition [16], $Z_g = 0$, appropriate to particles which are purely bound states of more basic fields; in this case we are presuming that ρ is to be regarded as a $q\bar{q}$ bound state [27].

The vanishing of the wave-function renormalization constant Z in the $\pi - \gamma$ transition element is another way of understanding how (28) emerges. Thus the full inverse (off-diagonal) vector meson propagator is

$$\Delta^{-1(\rho\gamma)}_{\mu\nu} = (-k^2 g_{\mu\nu} + k_\mu k_\nu) [Z + g_\rho^2 \Pi^{(\rho\gamma)}(k^2, m_q^2)], \quad (35)$$

and Z is normally taken to cancel the infinite part of the self-energy:

$$Z = 1 - g_\rho^2 \Pi^{(\rho\gamma)}(0, m_q^2). \quad (36)$$

Setting $Z = 0$, we recover precisely (28) in the chiral limit or $g_\rho = 2\pi$, again.

The other meson interactions arise from quark loops as they do through the gauge principle (with identical zero vertex renormalization constants) and thus it is rather easy to read off from (33) what they will be. In particular the transition amplitude $A_1 \rightarrow \rho\pi$ is found by substituting the induced vacuum expectation value $\langle\sigma\rangle = f_\pi$, producing the interaction $4g_\rho^2 f_\pi \vec{A}_1 \cdot \vec{\rho} \times \vec{\pi}$ and the decay rate

$$\Gamma_{A_1^+ \rho^+ \pi^0} = p(4g_\rho^2 f_\pi)^2 / 8\pi m_{A_1}^2 \simeq 250 \text{ MeV}, \quad (37)$$

for $m_{A_1} \simeq 1260 \text{ MeV}$, $p \simeq 620 \text{ MeV}$ and $f_\pi \simeq 90 \text{ MeV}$, not incompatible with experiment [17].

Next we turn to dynamical generation of the vector meson masses. Although current conservation suggests that the ρ mass may be zero (because of the gauge invariant form (35) of the two-point function and the strong analogy with vacuum polarization in QED), we should not jump to such a conclusion without examining the *full* self-energy and this includes the contributions from π , ρ and A_1 intermediate states. The various contributions are depicted in Fig. 9, producing the (diagonal) inverse ρ propagator,

$$\Delta_{\mu\nu}^{-1(\rho\rho)} = (-k^2 g_{\mu\nu} + k_\mu k_\nu) [Z + g_\rho^2 (\Pi^{(q\bar{q})} + \Pi^{(\pi\pi)} + \Pi^{(A_1\pi)} + \Pi^{(\rho\rho)} + \Pi^{(A_1 A_1)})]. \quad (38)$$

Since Higgs-like vector transversality still holds for (38) even on the ρ mass shell, the lhs of (38) must vanish. But to seek a zero on the rhs of (38) when $k^2 = m_\rho^2$, we must also require the $Z = 0$ compositeness condition [16]. Collecting the various terms and making use of (36), we must check that

$$0 = 1 - 4ig_\rho^2 \int_0^1 d\alpha \int \bar{d}^4 p \left[\frac{(1-2\alpha)^2}{[p^2 + m_\rho^2 \alpha(1-\alpha)]^2} + \frac{2(2g_\rho f_\pi)^2}{m_\rho^2 [p^2 - m_{A_1}^2 \alpha + m_\rho^2 \alpha(1-\alpha)]^2} \right. \\ \left. - \frac{22/3}{[p^2 - m_\rho^2 + m_\rho^2 \alpha(1-\alpha)]^2} - \frac{22/3}{[p^2 - m_{A_1}^2 + m_\rho^2 \alpha(1-\alpha)]^2} \right]. \quad (39)$$

The unity corresponds to the quark contribution; the second term, also positive, is that from a scalar massless particle [28]; the third term arises through the induced $\rho A_1 \pi$ coupling in (33), while the fourth and fifth terms are *negative* and associated with the purely vectorial contributions, including the famous factor of $11C_2/3$ that plays such an important role in asymptotic freedom [29].

Because all of the above integrals are just logarithmically divergent and scaled to the gap equation (4) or (31), with an implied cut-off $\Lambda \sim 750 \text{ MeV}$, a consistent procedure, already used to evaluate (32), is to reexpress (39) as

$$0 = 1 + \frac{g_\rho^2}{4\pi^2} \int_0^1 d\alpha \left[(1-2\alpha)^2 \left(\ln \left(1 - \frac{\Lambda^2}{m_\rho^2 \alpha(1-\alpha)} \right) - \frac{\Lambda^2}{\Lambda^2 - m_\rho^2 \alpha(1-\alpha)} \right) \right]$$

$$\begin{aligned}
& + \frac{8f_\pi^2 g_\rho^2}{m_\rho^2} \left(\ln\left(1 + \frac{\Lambda^2}{m_{A_1}^2 \alpha - m_\rho^2 \alpha(1 - \alpha)}\right) - \frac{\Lambda^2}{\Lambda^2 + m_{A_1}^2 \alpha - m_\rho^2 \alpha(1 - \alpha)} \right) \\
& - \frac{22}{3} \left(\ln\left(1 + \frac{\Lambda^2}{m_\rho^2(1 - \alpha(1 - \alpha))}\right) - \frac{\Lambda^2}{\Lambda^2 + m_\rho^2(1 - \alpha(1 - \alpha))} \right) \\
& - \frac{22}{3} \left(\ln\left(1 + \frac{\Lambda^2}{m_{A_1}^2 - m_\rho^2 \alpha(1 - \alpha)}\right) - \frac{\Lambda^2}{\Lambda^2 + m_{A_1}^2 - m_\rho^2 \alpha(1 - \alpha)} \right) \Bigg].
\end{aligned} \tag{40}$$

Taking the masses to be physical, with $\Lambda \simeq 750$ MeV, we may evaluate the integrals numerically as a function of Λ/m_ρ and search for a zero; in this way we estimate the ρ mass to be about 650 MeV. The interpretation of these computations is that the vector mesons do indeed develop masses dynamically of the right magnitude. Note that the dynamical consequence of generating a rho mass via Eqns. (38)-(40) in one-loop order is already simulated by the KSRF relation [30]. The latter holds in tree-order for our dynamically induced LSM which also generates the VMD relations via $Z = 0$ conditions.

Rather than repeat this (somewhat tedious) process for the axial A_1 meson, we observe from the third term of (33) that for a non-zero m_ρ ,

$$m_{A_1}^2 = m_\rho^2 + (2g_\rho f_\pi)^2. \tag{41}$$

Invoking the numerically accurate KSRF relation [30], $m_\rho^2 \simeq 2g_\rho^2 f_\pi^2$, we may conclude that

$$m_{A_1} \simeq \sqrt{3}m_\rho \simeq 1300 \text{ MeV}, \tag{42}$$

close to experiment but some way from the prediction $m_{A_1} = \sqrt{2}m_\rho$ that comes from spectral-function sum rules [31].

5 Vector meson dominance revisited

Having completed the dynamical generation of the gauged chiral quark model, we will end by commenting on the (extremely successful) VMD picture. Not only is VMD universality a consequence of the bootstrap mechanism, but the tree structure of all VMD graphs then becomes manifest since quark loops bootstrap to trees. Furthermore $g_{\rho\pi\pi} \simeq g_\rho$ is roughly satisfied by the theoretically derived value $g_\rho \simeq 2\pi$ in the chiral limit.

Concerning the $\rho - \gamma$ analogy of VDM, the relation between the two is governed by the quark loop, aside from coupling constants; in particular an examination of the quark loops for the processes $\rho \rightarrow \pi\gamma$ and $\pi^0 \rightarrow \gamma\gamma$ shows that the associated amplitudes [32] determine the empirical g_ρ/e coupling ratio [33]:

$$g_\rho/e = |2F_{\rho\pi\gamma}/F_{\pi^0\gamma\gamma}| \simeq 17.8 \tag{43}$$

using the measured rates⁹ $\Gamma_{\rho\pi\gamma} \simeq 67$ keV, $\Gamma_{\pi^0\gamma\gamma} \simeq 7.7$ eV. Again this ratio is close to the measured $g_{\rho e\bar{e}}$ value and fine structure constant:

$$g_\rho/e \simeq 5.03/0.3028 \simeq 16.6 \quad (44)$$

Likewise the vertices $A_1\rho\pi$ and $A_1\gamma\pi$ are VMD related and both contain a common gauge-invariant kinematic factor $(k.k'g_{\mu\nu} - k_\mu k'_\nu)$. In this case [34] one finds

$$g_\rho/e = |F_{A_1\rho\pi}/F_{A_1\gamma\pi}| \sim 15, \quad (45)$$

using the observed rates $\Gamma_{A_1^+\rho^+\pi^0} \sim 250$ MeV and $\Gamma_{A_1\pi\gamma} \simeq 640$ keV. The approximate agreement between the three ratios (43) - (44) emphasizes the (quark loop) $\rho - \gamma$ analogies of VMD.

Finally we compare the measured [35] pion charge radius $r_\pi = (0.66 \pm 0.02)$ fm with the gauged CQM and VMD predictions. The former CQM quarkloop is known to give [36]

$$r_\pi^2 = N_c/(2\pi f_\pi)^2 = 1/m_q^2 \simeq (0.61\text{fm})^2, \quad (46)$$

in the chiral limit, while the latter VMD value is

$$r_\pi^2 = 6/m_\rho^2 \simeq (0.63\text{fm})^2. \quad (47)$$

Suffice it to say that the measured radius lends further support to the gauged CQM and the compatible VMD picture.

In fact the entire scheme presented here, with dynamically generated (chiral limit) couplings $g = 2\pi/\sqrt{3}$, $g_\rho = 2\pi$ and masses $m_q = 2\pi f_\pi/\sqrt{3} \simeq 325$ MeV, $m_\rho \sim 750$ MeV and $m_{A_1} \simeq \sqrt{3}m_\rho$, along with the induced $\rho\pi\pi$ and $A_1\rho\pi$ vertices, are all consistent with the data.

6 Summary

In this paper we have started from the simple chiral quark model (2) where all bare parameters vanish and dynamically generated the entire sigma model Lagrangian in Sections 2 and 3 by working to one-loop order. As a bonus we obtained we obtained the meson-quark coupling $g = 2\pi/\sqrt{3}$ (a sizeable value) and sensible quark and sigma mass values. Then in Section 4 we gauged the scheme (again with zero bare vector masses) to include the vector meson interactions. Here we found the chiral-limiting quark coupling to be $g_\rho = 2\pi$ and got sensible masses for the vectors ρ and A_1 , as well as sensible interactions to the other mesons. Lastly, in section 5, we showed that the gauged CQM recovers the entire structure of (tree-level) VMD. The importance of bootstrapping loop graphs into tree graphs for dynamically generated field theories cannot be overstressed. This arises from $Z = 0$ conditions for fields such as σ and ρ which formally appear as elementary but are in fact bound states.

In hindsight we see that quadratically divergent tadpole graphs, (determined by dimensional regularization) are vital for studying the dynamical generation of the LSM field theory. Even though the sum over all tadpole graphs is zero, the individual contributions do not vanish by themselves; our procedure ensures that the Goldstone pion mass vanishes by guaranteeing that the quark, pion and σ bubble plus tadpole sums are zero *separately* [5]. The whole structure is tightly-knit and self-consistent.

7 ACKNOWLEDGEMENTS

RD acknowledges partial support from the Australian Research Council. MDS appreciates the hospitality of the University of Tasmania and the partial support of the U.S. Department of Energy. Both authors thank R. Tarrach for enlightening comments and A. Bramon for prior discussions.

References

- [1] S. Weinberg, Phys. Rev. Lett. **65** (1990) 1177.
- [2] M. Gell-Mann and M. Levy, Nuovo Cim. **16** (1960) 705; see also V. deAlfaro, S. Fubini, G. Furlan and C. Rossetti, Chap. 5 in *Currents in Hadron Physics* (North Holland, Amsterdam, 1973).
- [3] Y. Nambu and G. Jona-Lasinio, Phys. Rev. **122** (1961) 345.
- [4] T. Eguchi, Phys. Rev. **D14** (1976) 2755; **D17** (1978) 611. Also see D. Lurié and A.J. Macfarlane, Phys. Rev. **136** (1964) B816.
- [5] T. Hakioglu and M. D. Scadron, Phys. Rev. **D42** (1990) 941; *ibid.* **D43** (1991) 2439.
- [6] M. D. Scadron, Mod. Phys. Lett. **A7** (1992) 479; Phys. At. Nucl. **56** (1993) 1595.
- [7] such as vector meson dominance universality and the mended chiral symmetry equation, $\Gamma_\sigma = 9\Gamma_\rho/2$.
- [8] J. Bijnens, C. Bruno and E. deRafael, Nucl Phys. **390** (1993) 501; B. Holdom, J. Terning and K. Verbeek, Phys. Lett. **B245**, (1990) 612.
- [9] J. Goldstone, Nuovo Cim. **19** (1961) 154; J. Goldstone, A. Salam and S. Weinberg, Phys. Rev. **127** (1962) 965.
- [10] We need not include logarithmically divergent (σ and $\vec{\pi}$ mediated) quark self-energy graphs in Fig.1b because direct calculation shows that they actually cancel on the quark mass shell due to chiral symmetry. However

we must not consider quadratically divergent σ and π loop tadpole graph contributions because pure meson $\pi\pi\sigma$ and $\sigma\sigma\sigma$ couplings do not appear in the primary Lagrangian (2). We will consider these additional tadpoles after dynamical generation of the LSM.

- [11] Our notation is $\bar{d}^4 p = d^4 p / (2\pi)^4$ and we naturally just assume two flavours throughout.
- [12] The emergence of an expectation value f_π , via $\delta f_\pi = f_\pi$ is virtually the same equation. Basically there occurs a cancellation between the physical quantity and the quantum correction, as happens for the fermion mass; the former is positive and the latter is negative. As such, eqs.(5) and (9) arise as counter-term masses.
- [13] see e.g. reviews by R. Delbourgo, Repts. Prog. Phys. **39** (1976) 345; G. Leibbrandt, Rev. Mod. Phys **47** (1975) 849.
- [14] B. W. Lee, p.12, *Chiral Dynamics* (Gordon and Breach, NY, 1972).
- [15] These integrals are dominated by their divergences and are thus being evaluated at zero external momenta.
- [16] A. Salam, Nuovo Cim. **25** (1962) 224; S. Weinberg, Phys. Rev. **130** (1963) 776.
- [17] Particle Data Group, K. Hikasa et al, Phys. Rev. **D45 II** (1992) 1.
- [18] P. Estabrooks, Phys. Rev. **D19** (1979) 2678; N. Biswas *et al*, Phys. Rev. Lett. **47** (1981) 1378; T. Akesson et al, Phys. Lett. **B133** (1983) 241; N. Carson *et al*, Phys. Rev. **D28** (1983) 1586; A. Courau *et al*, Nucl. Phys. **B271** (1986) 1; M. Svec *et al*, Phys. Rev. **D45** (1992) 55.
- [19] S. Adler, Phys. Rev. **177** (1969) 2426; J. Bell and R. Jackiw, Nuovo Cim. **60** (1969) 47.
- [20] extracting out the standard kinematic factor $\epsilon_{\mu\nu\alpha\beta} k'^\mu k^\nu \epsilon'^\alpha \epsilon^\beta$.
- [21] J. Steinberger, Phys. Rev. **76** (1949) 1180.
- [22] S. Coleman and E. Weinberg, Phys. Rev. **D7** (1973) 1888; see also sec 13.9 in D. Bailin and A. Love, *Introduction to Gauge Field Theory* (Adam Hilger, IOP, 1986)
- [23] B. Holdom, Phys. Rev. **D45** (1992) 2534.
- [24] L. H. Chan, Phys. Rev. Lett. **39** (1977) 1125; *ibid* **55** 1985 (21); V. Novozhilov, Phys. Lett. **B228** (1989) 240.
- [25] J. J. Sakurai, Ann. Phys. NY **11** (1960) 1.

- [26] because $g_{\rho\pi\pi}^2/4\pi \simeq 2.9$, given the observed decay rate $\Gamma_\rho \simeq 150$ MeV.
- [27] We invoked the same $Z_g = 0$ condition when we bootstrapped the $g' = g_{\sigma\pi\pi}$ coupling in the linear sigma model via a quark loop.
- [28] That is why we have disregarded the pion tadpole bubble—zero by dimensional regularization.
- [29] See e.g. I. J. R. Aitchison and A. G. Hey, *Gauge Theories in Particle Physics* p.297 (Adam Hilger, Bristol, 1989).
- [30] K. Kawarabayashi and M. Suzuki, Phys. Rev. Lett **16** (1966) 255; Riazuddin and Fayyazuddin, Phys. Rev. **147** (1966) 1071. This KSRF relation can also be derived dynamically by again demanding vector current conservation together with VMD (the latter already a consequence of the LSM). See J.J. Sakurai, Phys. Rev. Lett. **17** 1966 (552) to obtain $m_\rho \approx \sqrt{2}f_\pi \tilde{g}_\rho \approx 750$ MeV, given the dynamically generated ρ coupling $\tilde{g}_\rho = \sqrt{g_\rho g_{\rho\pi\pi}} \approx 5.7$.
- [31] S. Weinberg, Phys. Rev. Lett. **18** (1967) 507.
- [32] multiplying the kinematic factor $\epsilon_{\mu\nu\rho\sigma} k'^\mu k^\nu \epsilon'^\rho \epsilon^\sigma$, which is automatically gauge-invariant.
- [33] M. Gell-Mann, D. Sharp and W. Wagner, Phys. Rev. Lett. **8** (1962) 261.
- [34] A. Bramon and M. D. Scadron, EuroPhys. Lett. **19** (1992) 663.
- [35] S. Amendolia *et al*, Phys. Lett. **B146** (1984) 116; *ibid* **B178** (1986) 435.
- [36] R. Tarrach, Z. Phys. **C2** (1979) 221; S. Gerasimov, Sov. J. Nucl. Phys. **29** (1979) 259.

Fig.1a Logarithmically divergent quark loop for f_π .

Fig.1b Quadratically divergent graph for m_q .

Fig.2a Quark loop contribution to the pion self-energy.

Fig.2b Quark tadpole contribution to the pion self-energy.

Fig.3a Quark loop contribution to the sigma self-energy.

Fig.3b Quark tadpole contribution to the sigma self-energy.

Fig.4a Quark loop contribution to the $\sigma\pi\pi$ vertex.

Fig.4b Quark loop contribution to the $\sigma\sigma\sigma$ vertex.

Fig.5 Quark loop contribution to the quartic meson vertices.

Fig.6 The total tadpole contribution to $\langle\sigma'\rangle$.

Fig.7 Quark loop contribution to the $\rho - \gamma$ transition amplitude.

Fig.8 Quark loop contributions to the $\rho\pi^+\pi^-$ vertex.

Fig.9 Quark, pion, ρ and A_1 contributions to the ρ meson self-energy.

Fig. 1

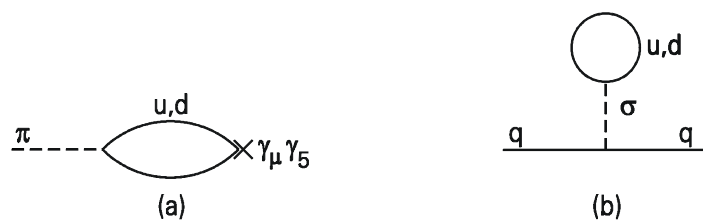


Fig. 2

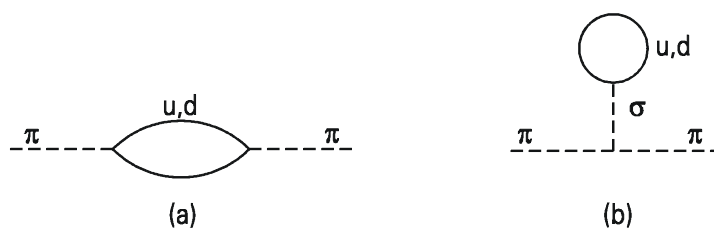


Fig. 3

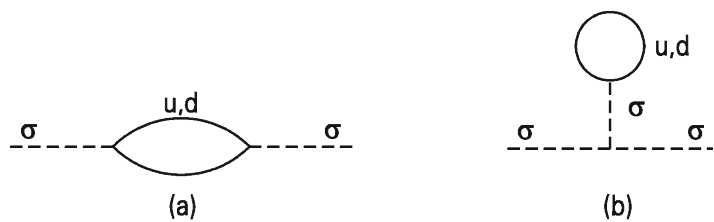


Fig. 4

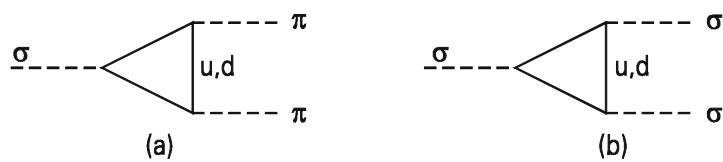


Fig. 5

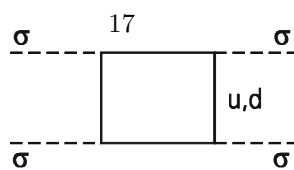
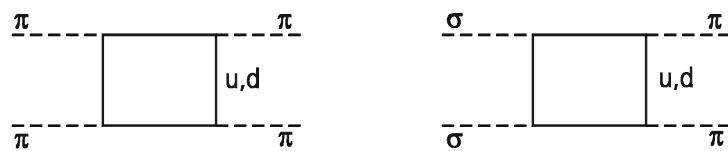


Fig. 6

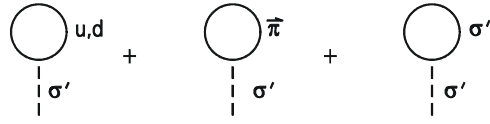


Fig. 7

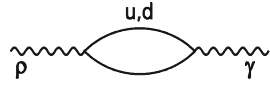


Fig. 8

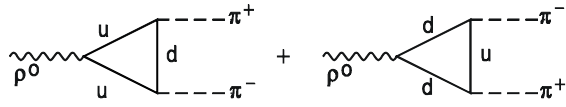


Fig. 9

